Shock Wave Boundary Layer Interactions at Compression Ramps Examined by Converged Statistical Schlieren

Zhengzhong Sun[1,*], Tian Gan[2], Yun Wu[2]
1: Dept. of Mechanical Engineering and Aeronautics, City, University of London, UK
2: School of Mechanical Engineering, Xi'an Jiaotong University, UK
* Correspondent author: zhengzhong.sun@city.ac.uk

Keywords: SWBLI, High-Speed Schlieren, Flow Unsteadiness

ABSTRACT

Shock wave boundary layer interactions at compression ramps have been examined by high-speed schlieren. A total of six ramps with angles ranging from 20 deg to 30 deg, the ramp angle effect on the SWBLI is thus studied. The present high-speed schlieren with a frame rate of 20 kHz generates a large ensemble of 9000 images, which secures the convergence of the statistics of the schlieren intensity. The rms of the schlieren intensity is of great interest, as it enables visualisation of the flow features that are not observable in the raw schlieren images, such as the corner separation/low momentum region, the spot of strong flow unsteadiness right after the shock wave and the location of the peak fluctuation over the ramp. Through the present systematic experimental investigation of SWBLI, the high-speed schlieren is demonstrated to be of great capability for SWBLI study.

1. Introduction

Shock wave boundary layer interaction (SWBLI) is an important phenomenon in the transonic, supersonic, and hypersonic regime. Ample researches on SWBLI have contributed to the profound understanding on this phenomenon since the very pioneering works on this topic in the 1950s [1]. The great amount of attentions that attracted to SWBLI is directed by its induced adverse effects, namely flow separation, unsteady nature, and turbulence generation [2]. Flow separation is an unexpected feature in any aerodynamic applications, and it naturally reduces aerodynamic efficiency and induces drag. The flow separation in the interaction system is of prominent unsteady nature, which is usually referred to as the low-frequency unsteadiness in the band of 100~1000 Hz. The flow unsteadiness will result in additional structural considerations and flight control issues. The occurrence of SWBLI not only affects the local region, but also influences the region downstream of the interaction. The flow downstream of SWBLI features much higher turbulence intensity, which is harmful for the devices located at downstream. For example, in the case of highly-loaded gas turbine, the SWBLI in the turbine blade channel generates higher

turbulence in the downstream portion of the channel. Heat transfer is thus enhanced, and the blades, resultantly, are subject to severe heat load.

Flow control strategies are usually devised to alleviate these adverse effects. But appreciation of the very fundamental physics associated with the SWBLI is of vital importance before any flow control is applied. The present experimental research is a continuing effort dedicated to the unsteady aspect of the SWBLI. The SWBLIs on compression ramps are chosen for investigation as it is commonly seen in applications, such as supersonic inlet and some external surfaces in hypersonic applications. To differ from the previous reported works on individual compression ramps, the present study investigates the SWBLIs at several compression ramps ranging from 20 degrees to 30 degrees with an increment of 2 degrees. Hence a total of 6 ramps are measured in the wind tunnel. High-speed schlieren is used as the primary flow diagnostic method. Some detailed flow structures are analysed by taking full advantage of the large data ensemble recorded at high-frame rate. In the remainder of this paper, the experimental setup is first presented. In the discussion of the results, the flow structures and the frequency characteristics are carefully examined. Finally, conclusions are drawn.

2. Experimental Setup

A suction-type supersonic wind tunnel is used as the flow facility. The flow is driven by the pressure difference between the ambient and the vacuum in the tank downstream of the test section. This wind tunnel can generate Mach numbers of 2.0 and 3.0 by using different contoured nozzles. In the present experiment, the Mach 2.0 nozzle is used. The nozzle has a circular cross-section. Its outlet has a diameter of 30 mm. The supersonic free jet will go through the test chamber. The test chamber has a diameter of 1.5 m, which is deemed large enough to avoid the wall interference towards the jet flow. The ramp model is placed on the flat plate. In the present experiments, a base plate with flat surface is used, the ramps are installed 225 mm downstream of the flat plate's leading edge. Therefore, a flat surface of about 225 mm is used to develop the boundary layer. Inspection of the schlieren images finds that the boundary layer thickness is about 0.8 mm at the location of the ramp corner. Hence the Reynolds number is estimated to be 28,900 based on the boundary layer thickness. A total of 6 ramps with angles ranging from 20 degrees to 30 degrees are available, such that how SWBLI is affected by the ramp angle can be examined. The model is mounted onto the bottom of the test chamber through a vertical steel sting. It will be realised later that this mounting arrangement has low-frequency vibration (less than 100 Hz).

3. Results and Discussion

3.1 The instantaneous schlieren snapshot

Instantaneous schlieren snapshots for each ramp are shown in figure 1. The origin of the axis is placed at the ramp corner. The ramp height h is chosen as the length scale for spatial normalization. The most prominent structures in the flow are the shock wave and the turbulent region right after the shock wave and over the ramp. The incoming boundary layer is very thin and appears as the darker strip over the flat surface. Increasing the ramp angle generates a stronger shock wave. According to the inviscid theory, the shock wave will become detached from flow deflection of 24 degrees. However, the present visualizations reveal that the viscous effect alleviates the flow deflection, and all the shock waves are attached despite the ramp angle being larger than the theoretical deflection angle.

Increasing the ramp angle makes the interaction region extend further upstream. In the present discussion, the interaction region is defined as the region between the inviscid shock impingement point and the ramp corner. In the case of 20-deg ramp, the interaction region has a length of about L/h=0.57, and it eventually grows to L/h=1.47 for the ramp of 30 degree.

The schlieren technique is a qualitative flow visualization method and cannot reveal any information of flow direction. It is usually deemed that the separation bubble is bounded by the separation shock wave (SSW) and the reattachment shock wave (RSW). Comparing the schlieren images in figure 1, the SSW and RSW are separated with longer distance over the larger ramps, suggesting an increased separation region. The RSW becomes stronger over larger ramp angles. However, the RSW is not as focused as the SSW, which is perhaps due to the fact that the flow deflection right after the separation bubble is less abrupt.

The near wall flow obtains stronger turbulent intensity over the ramp surface, which is a well-recognised outcome of SWBLI at compression ramps. The highly turbulent region has larger height over the ramp with larger angle, where stronger SWBLI is present. The spatial gradient of the schlieren intensity $\|\nabla I\|$ is also calculated. An appropriate magnitude is chosen to visualise the prominent structures of the SWBLIs, and they are shown figure 2, where the shock waves and the induced turbulence are clearly shown. In the next section, the strength of turbulence intensity will be examined through the statistics of schlieren intensity.

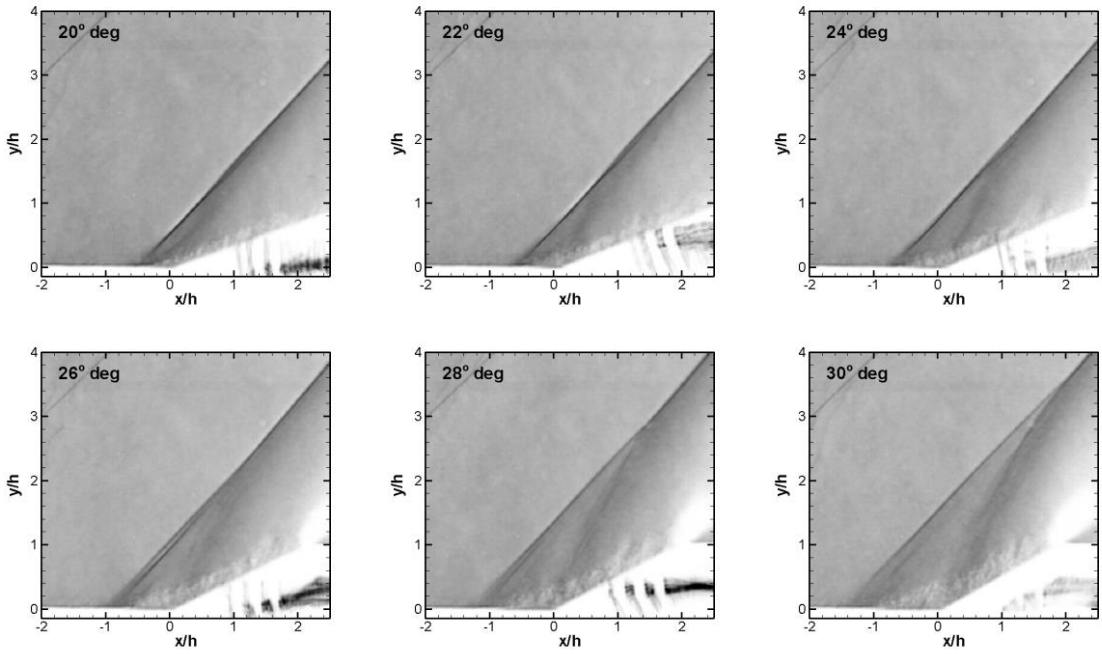

Fig. 1 Schlieren snapshots for the SWBLIs at the compression ramps.

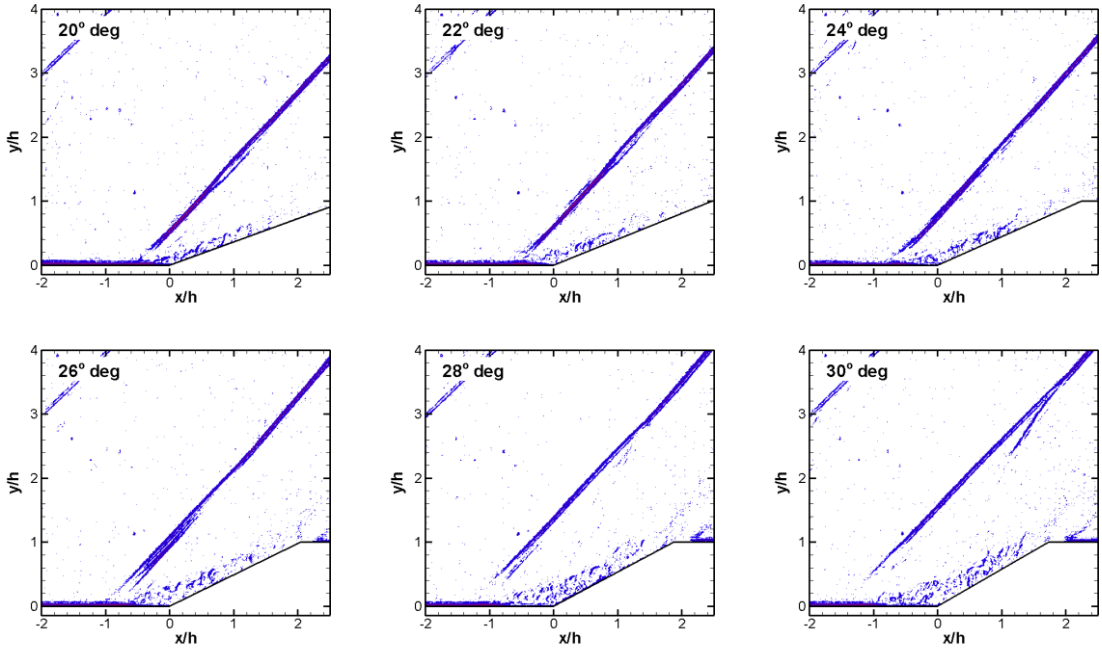

Fig. 2 The SWBLIs visualised by the gradient of the schlieren intensity.

3.2 The statistics of schlieren images

The use of ultra-high-speed camera (UHSC) enables collection of a very large ensemble of images. It is a great advantage for wind tunnel of very short period of operation. Taking full benefit of this UHSC, the present data ensemble for each ramp contains a total of 9,000 images, which is

expected to secure the convergence of the statistical quantities, including the mean and rms of the schlieren intensities. The convergence for both quantities are examined through the residuals for ensembles with increasing number of images, which are shown in figure 3. The residuals for all the ramp cases are included, shown as the dots with different colours. The solid line is the mean convergence curve averaged among all the ramp cases using the same number of snapshots. The residuals for the mean schlieren intensity is already blow 1 count after 300 images, while the residual using the entire ensemble is far below 1 count. Hence convergence for the mean schlieren intensity can be concluded. The residual evolution for the rms of the schlieren intensity is represented in figure 3(b), where the solid line is the same as that in figure 4(a), namely the averaged residual curve for the mean schlieren intensity for all the ramps. It is clear that the convergence of the rms of the intensity is slower and requires nearly 1000 images to reach a level of $\varepsilon_{rms}<1$. Hence, the present size of image ensemble is also sufficient to secure a converged rms intensity field.

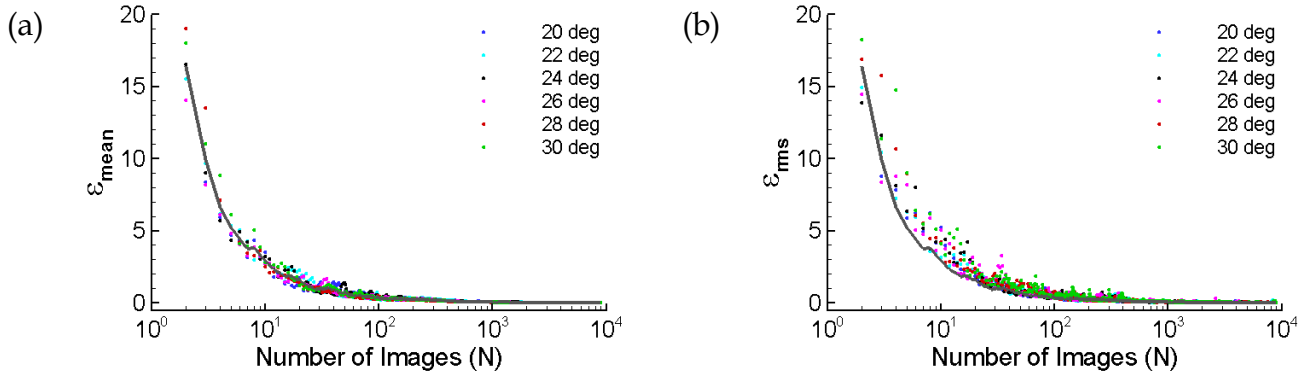

Fig. 3 The convergence history of mean and rms of schlieren intensity field.

The averaged schlieren intensity fields are shown in figure 4. They are, to some extent, equivalent to the schlieren images captured with an exposure time of 9000/20=450 ms. The region featured with shock induced turbulence shows up as a bright strip over the ramp. The small scale turbulent eddies that visualised in the instantaneous snapshots are no longer observable as they all together contribute to mean intensity of the shock induced turbulent. The occurrence of the reattachment shock wave follows the trend as observed in the instantaneous snapshots. The increase of the interaction length has been discussed through the instantaneous snapshot. The mean interaction length is also measured and summarised in figure 5. The growth of L is not linear with respect to the ramp angle. A steeper increase of L can be found in the ramps with angles of 24 and 26 degrees, which are beyond the flow deflection angles for attached shock wave in the theoretical inviscid case. The measured mean interaction length is also listed in Table 1.

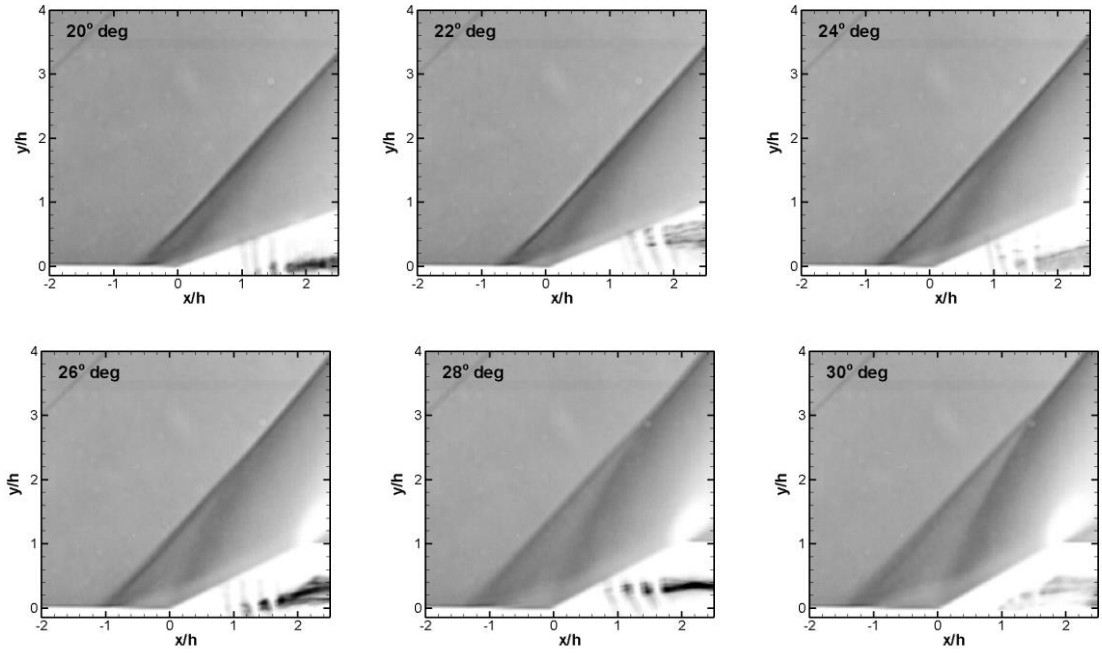

Fig. 4 The mean schlieren intensity fields for all the ramps.

Table 1 The mean interaction length in the SWBLIs.

Ramp angle [deg]	20	22	24	26	28	30
L/h	0.57	0.70	0.78	1.04	1.36	1.47

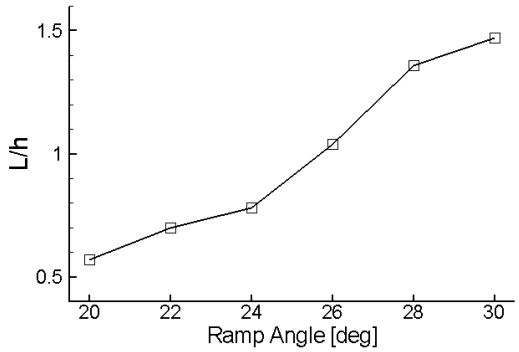

Fig. 5 The growth of the interaction length for different ramps.

It has been shown in figure 3 that the rms of the schlieren intensity Irms has reached convergence. The rms of the schlieren intensity for each ramp is going to be discussed. They are represented in figure 6. The shock wave and the turbulent region caused by the SWBLI are clearly visualised. The shock wave obtains much larger values of Irms, which is due to the fact that large value of I is present at the shock location and movement of shock wave makes the local schlieren

intensity to fluctuate. The concentration of the Irms is an indication of the mean shock location. However, only the higher portion of the RSW is visualised by the Irms, as the lower portion is comprised of weak compression waves, which coalesce into the RSW. So far, it can be concluded that only the focused shock wave can be visualised through the Irms. The turbulent region caused by SWBLI also features high Irms intensity, but its magnitude is one order smaller than that of the shock wave. The near-wall high Irms region starts immediately downstream of the SSW and extends over the ramp. The peak Irms can be found shortly after the ramp corner at x/h= 0.18 for the 20-deg ramp, and it moves further downstream for ramps with larger angles.

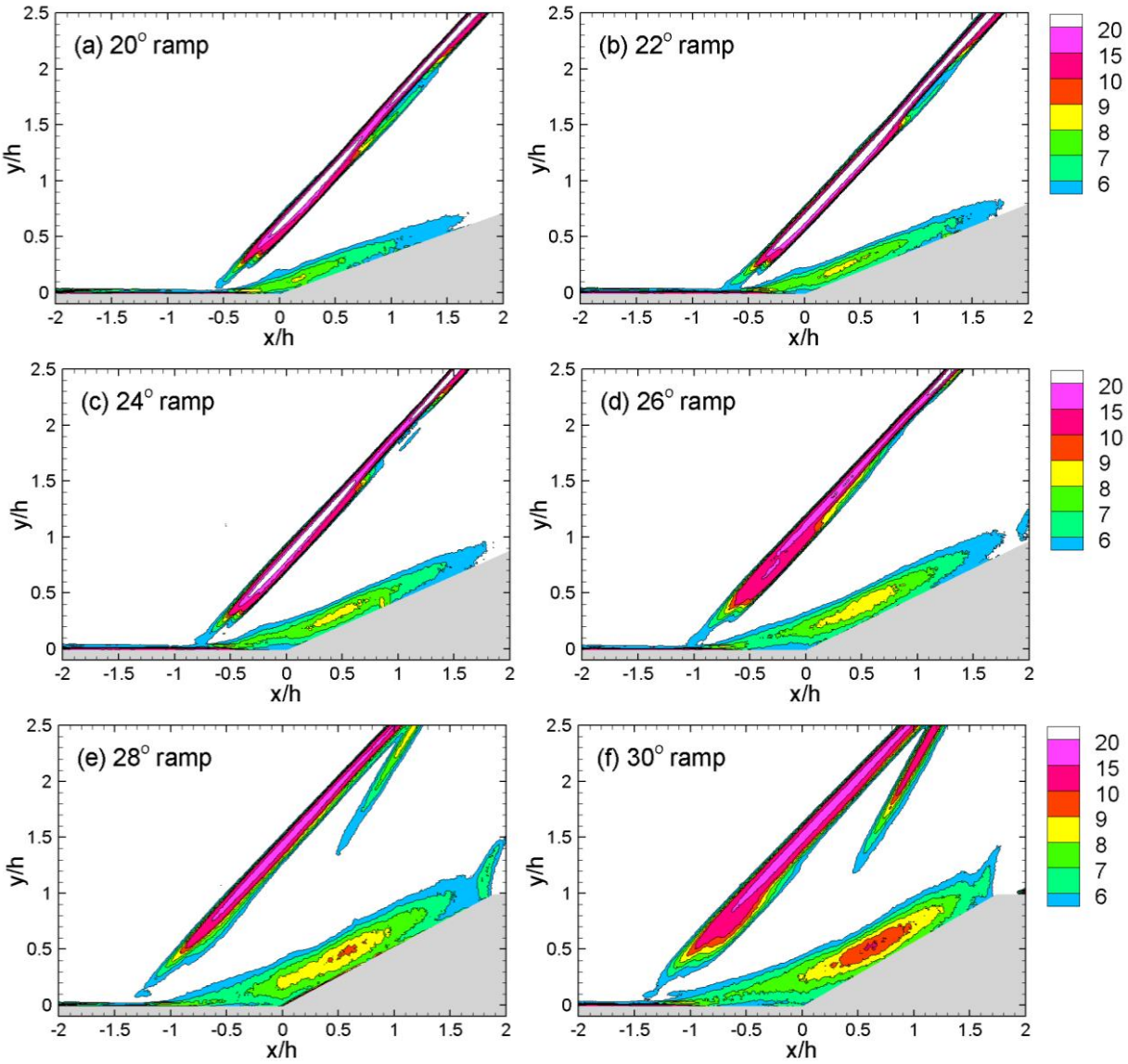

Fig. 6 The rms of schlieren intensity for the compression ramp flows.

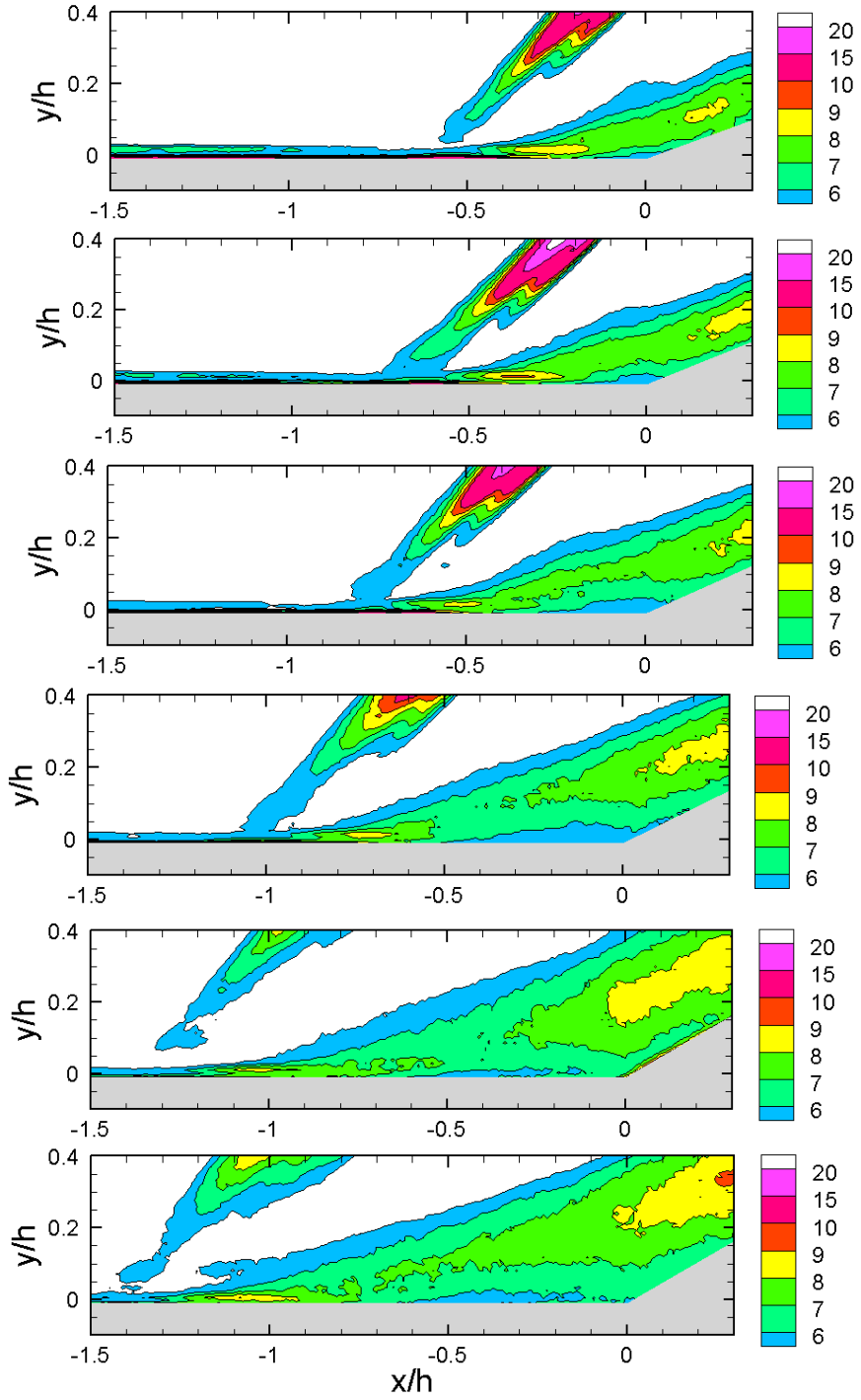

Fig. 7 The rms of schlieren intensity in the SWBLI region.

Since the schlieren image records the flow information using every pixel, hence allows high-spatial resolution. The SWBLI regions are enlarged in figure 7 for further observation. The thin boundary layer is represented by the stripe with I_{rms}=6. This close-up view gives better representation of the SWBLI region. Immediately downstream of the shock impingement, an elongated spot of I_{rms}=8~9 is produced and it has a streamwise extension of 0.2h. This spot of

higher I_{rms} is likely associated with the unsteadiness in the SWBLI. It is not immediately observable from the raw schlieren snapshots. Downstream of the spot and exactly at the corner of the compression ramp, the magnitude of I_{rms} is smaller. This region is inferred as the region of flow separation or of low-momentum if separation does not take place in the mean sense. With the increase of the ramp angle, this corner region of low I_{rms} grows in size. It extends mainly upstream from x/h = -0.15 to -0.5, while the end-point has only slight downstream movement. Therefore, the present visualisation is capable of revealing the flow features in the SWBLI that are not immediately available in the raw snapshots, such as the separation/low-momentum region at the ramp corner, the spot of high I_{rms} at the shock foot and the concentration of the near wall turbulent region over the ramp.

3.3 The Spectrum Analysis

The present recording rate (i.e. 20 kHz) is much higher than the well-known dominating low-frequency unsteadiness in the SWBLI (i.e. 100Hz~1000Hz), therefore spectrum analysis is possible for the shock wave oscillation associated with the low-frequency unsteadiness. Reviewing the schlieren recording also finds that the recording frequency is fast enough to deliver the time-resolved imaging for the shock wave. The time separation between two consecutive frames is 50 μs, which is, however, too large to resolve the temporal evolution of the turbulent eddies in the wall turbulence. As a result, the present high-speed schlieren is deemed suitable to study the spectrum of the shock wave oscillation.

The schlieren intensity at four heights, namely y/h=0.5, 1.0, 1.5 and 2.0, are selected to perform the FFT analysis. The resulted spectra within the four planes belonging to the 30-deg compression ramp are shown through the contours in figure 8, where the contours are coloured by the resulted intensity of FFT calculation. Note that only the result of 30-deg ramp is shown and discussed, as those for the other ramps share similar spectrum characteristics.

The spectrum of the separation shock is already resolved at y/h=0.5. The spectrum intensity terminates at around 1kHz. A lower bound around 100Hz is also expected. However, the lower bound of the shock wave spectrum does not terminate at 100Hz, instead it also features some very low frequency (<100Hz) motions, which are later understood as the frequency associated with model vibration, as the ramp model is mounted through a long cantilever type sting. This very low frequency component exists in the rest of the spectrum contours. The region from x/h=0 till the ramp surface is highlighted by intensified spectra till the end of the maximum achievable frequency. This region belongs to the near wall turbulent region over the ramp and it is likely to have characteristic frequency larger than 1kHz. Moving gradually further away from the wall, the intensity of the separation shock spectrum builds up gradually, as it also has a

tendency to terminate at slightly higher frequency, nearly 5kHz, which is apparently beyond the 100-1000 Hz band. The spectrum of the turbulent region over the ramp is also represented at y/h=1.0, but with a smaller thickness. In the same plane, the reattachment shock is about to appear, as weak traces of amplified intensity can be observed at x/h=0.2. The spectrum of the reattachment shock also obtains larger magnitudes at higher locations, and it terminates at an upper bound of 5kHz, which is also larger than the low-frequency band. This increased frequency is probably associated with the vortex shedding frequency in the turbulent shear layer over the ramp.

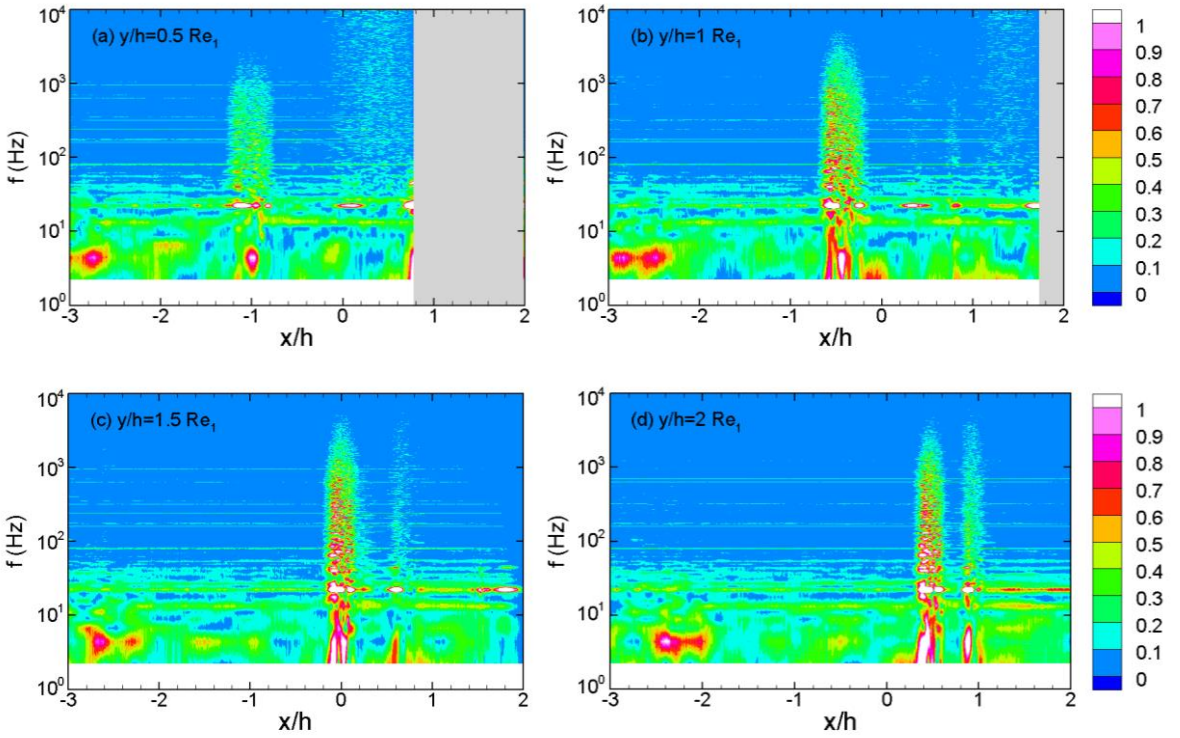

Fig. 8 The spectra of schlieren intensity for 30-deg ramp at y/h=0.5,1.0,1.5 and 2.

4. Conclusions

The present high-speed schlieren experiments successfully visualised the SWBLI phenomena taking place over compression ramps with ramp angles from 20 to 30 degrees. The flow pattern around the compression ramps and the shock wave organisation are clearly revealed. It is found that increasing the ramp pushes the interaction region upstream and generates a thicker turbulent layer over the ramp surface. Taking full advantage of the large schlieren image ensemble, converged mean and rms of the schlieren intensity field can be achieved. The mean intensity field reveals that the reattachment shock wave has weaker intensity than the separation

shock wave, while the rms intensity field offers more details that are not immediately observable in the raw schlieren snapshots, including the high Irms spot right after the shock impingement, the corner separation region/low momentum region, and the peak turbulent intensity location over the ramp. Spectrum analysis is finally carried out and the oscillations for the two shock waves are compared. The separation shock wave has maximum frequency of about 1kHz at a lower location of y/h=0.5, but its spectrum extends to a higher frequency of 5kHz. The spectrum of the reattachment shock wave, similarly, has a frequency band terminating towards 5kHz. The higher frequency beyond 1kHz is perhaps linked with the vortex shedding frequency at the turbulent shear layer over the ramp.

Acknowledgement

This project receives supports from UK EPSRC (EP/R013608/1), UK Royal Society International Exchange Program (IE150612), UK Royal Society Research Grant (RSG\R1\180236).

References

[1] Dolling DS (2001) Fifty years of shock-wave/boundary-layer interaction research: What Next?, AIAA J., 39(8):1517-1531.

[2] Humble RA, Elsinga GE, Scarano F, van Oudheusden BW (2009) Three-dimensional instantaneous structure of a shock wave/turbulent boundary layer interaction, J. Fluid Mech., 622:33-62.